Electronic Supplementary Material (ESI) for Journal of Materials Chemistry A.

Supporting Information

Heteroatom P filling activates intrinsic S atomic sites of few-layered $ZnIn_2S_4$ via modulation of H adsorption kinetics for sacrificial-free photocatalytic hydrogen evolution from pure water and seawater

Boon-Junn Ng,[a] Wei-Kean Chong,[a] Lutfi Kurnianditia Putri,[a] Xin Ying Kong,[b] Jingxiang Low,[a,c] Hing Wah Lee,[d] Lling-Lling Tan,[a] Wei Sea Chang,[e] Siang-Piao Chai[a,*]

Table S1. Composition of the artificial seawater.

Element	Amount (mg/L)	Element	Amount (mg/L)
Chloride	19230	Silicon	< 0.05
Sodium	10610	Iron	0.012
Sulfate	2485	Copper	0.0003
Magnesium	1390	Nickel	< 0.015
Potassium	398	Zinc	0.008
Calcium	409	Manganese	0.01
Carbonate	179	Molybdenum	0.01
Strontium	10	Cobalt	0.0004
Boron	7.6	Vanadium	< 0.015
Bromide	20	Selenium	< 0.019
Iodide	0.05	Rubidium	0.115
Lithium	0.26	Barium	< 0.05

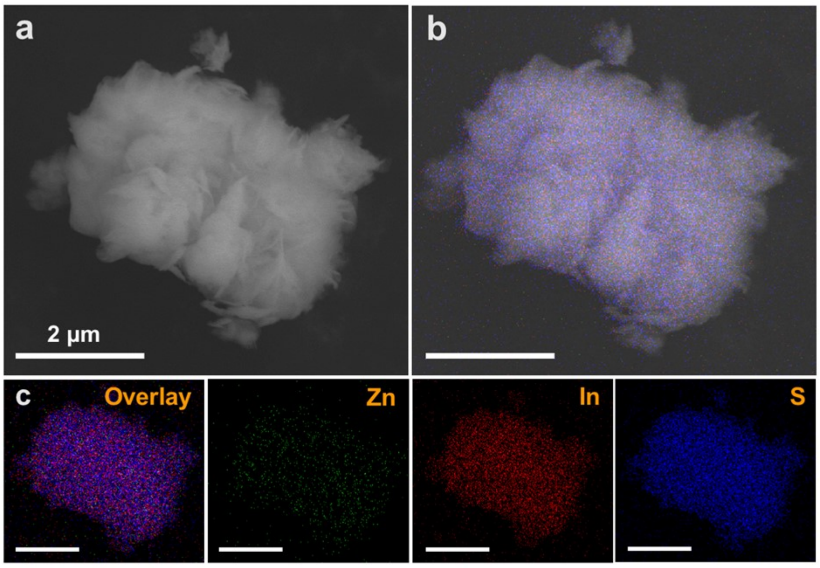

Fig. S1 Morphology and composition of pristine ZIS. (a) FESEM image and corresponding (b) false colored and (c) EDX elemental mapping of pristine ZIS (scale bar: 2 µm).

Table S2. Analytical data of energy-dispersive X-ray (EDX) spectroscopy of the P-doped samples.

Entry	Sample	P Atomic Percentage (at %)
1	ZIS-P100	3.08
2	ZIS-P200	6.97
3	ZIS-P300	10.89

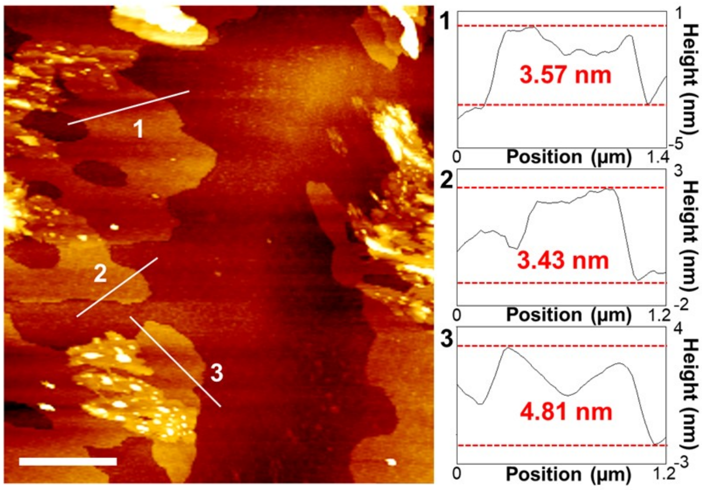

Fig. S2 AFM analysis. AFM image and corresponding height profile of ZIS (scale bar: 1 μm).

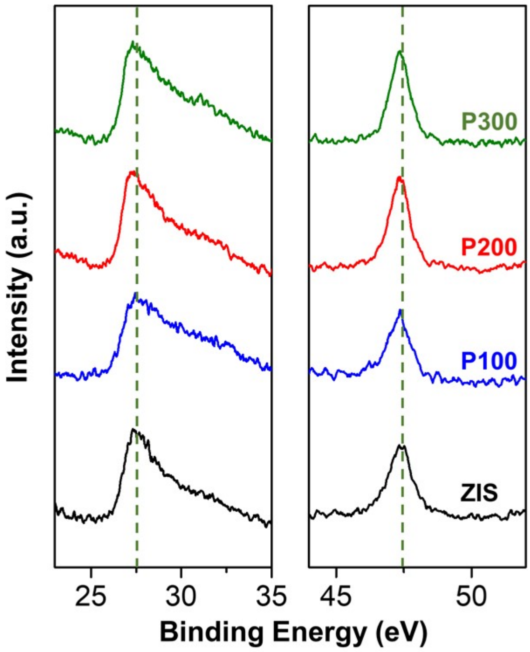

Fig. S3 XRD analysis. Enlarged XRD peaks showing (102) and (110) crystal planes of the respective samples.

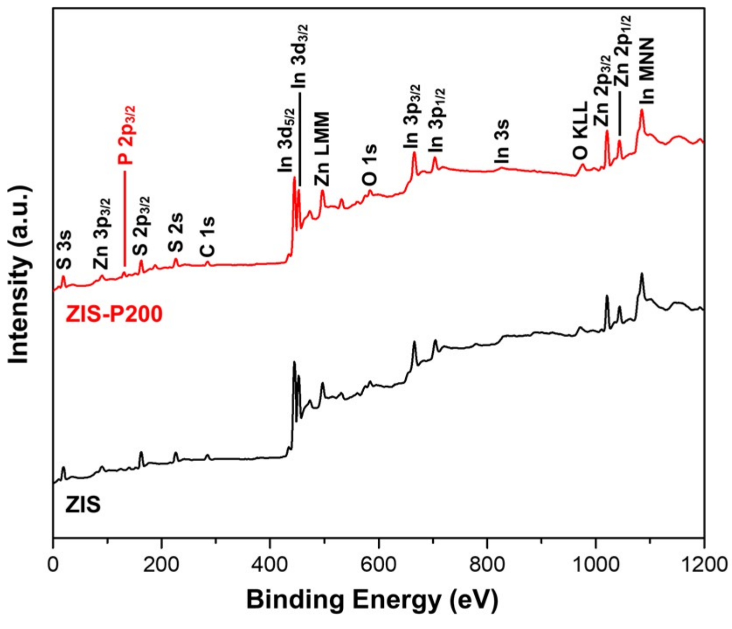

Fig. S4 XPS analysis. Full XPS spectra of ZIS and ZIS-P200.

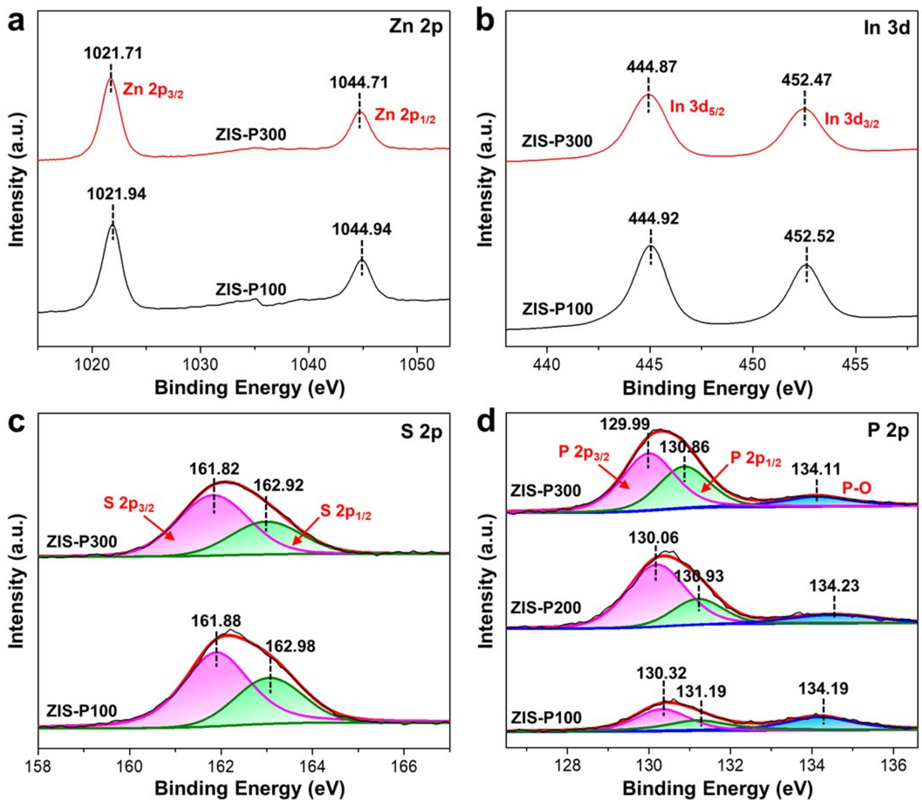

Fig. S5 XPS analysis on the effect of P content. (a) Zn 2p, (b) In 3d and (c) S 2p XPS spectra of ZIS-P100 and ZIS-P300. (d) P 2p XPS spectra of ZIS-P100, ZIS-P200 and ZIS-P300.

Table S3. Relative atomic ratio of ZIS and ZIS-P200 measured by XPS.

Entry	**Sample**	**Atomic Ratio (Normalized to Zn = 1)**		
		Zn	In	S
1	ZIS	1	2.13	3.94
2	ZIS-P200	1	2.19	3.30

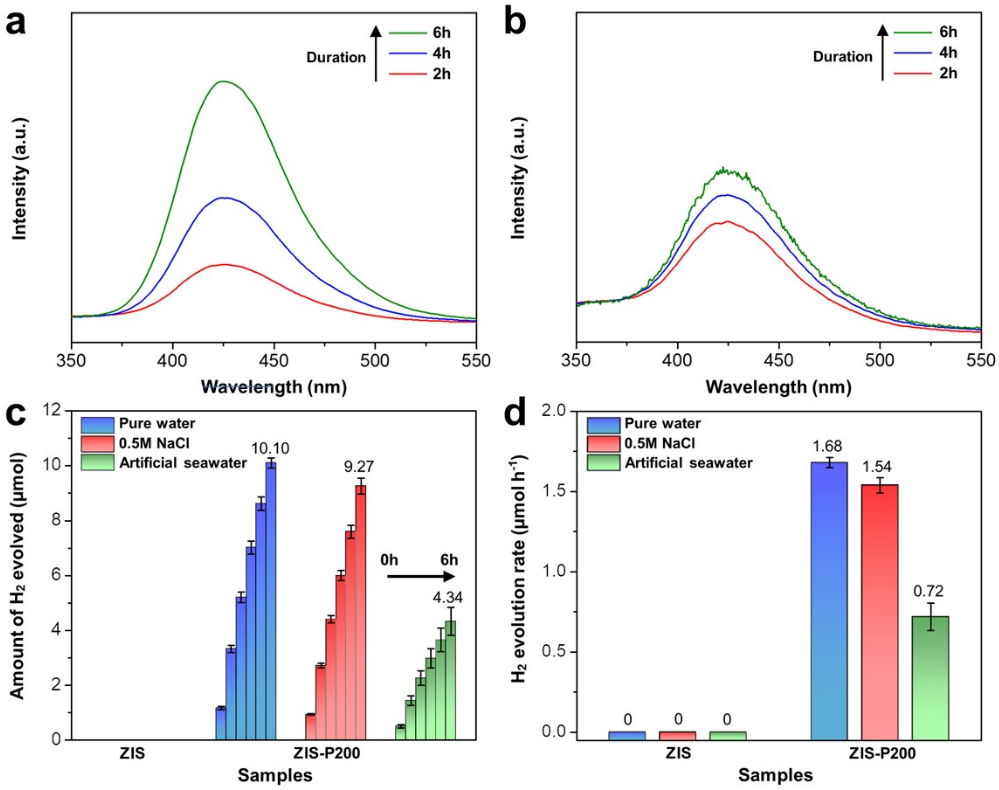

Fig. S6 Photocatalytic performance on pure water and seawater splitting. Time dependence of •OH trapping PL spectra for ZIS-P200 in (a) pure water and (b) 0.5 M NaCl under visible light irradiation. (c) Time courses of H_2 evolution and (d) corresponding H_2 yield of ZIS and ZIS-P200 in pure water, 0.5 M NaCl and artificial seawater under visible light irradiation.

Table S4. Comparison of photocatalytic HER performance from pure water and simulated seawater for single-component photocatalysts.

Photocatalyst	Co-catalyst	Reaction Condition	Performance	Ref.
ZIS-P200	-	DI water (60 mL); 350 W Xe lamp ($\lambda > 400$ nm)	H_2: 1.68 μmol h^{-1} AQY: 0.16% (420 nm)	This work
Ni-doped $ZnIn_2S_4$	-	DI water (45 mL); 300 W Xe lamp (AM 1.5)	H_2: 0.86 μmol h^{-1}	[S1]

P-doped $Zn_{0.5}Cd_{0.5}S_{1-x}$	-	DI water (120 mL); 500 W Xe lamp ($\lambda > 400$ nm)	H_2: 0.97 μmol h^{-1} AQY: 0.15% (420 nm)	[S2]
CdS	CoP and WS_2	DI water (100 mL); 300 W Xe lamp ($\lambda > 420$ nm)	H_2: 0.46 μmol h^{-1}	[S3]
P-doped CdS	CoP	DI water (20 mL); 3 × 30 W LED lamp ($\lambda > 420$ nm)	H_2: 1.16 μmol h^{-1}	[S4]
ZIS-P200	-	0.5 M NaCl (60 mL); 350 W Xe lamp ($\lambda > 400$ nm)	H_2: 1.54 μmol h^{-1}	This work
WO_2-Na_xWO_3 hybrid conductor	-	0.2 M phosphate-buffered saline (pH = 6) (10 mL); 1000 W Xe lamp (Full spectrum)	H_2: ~0.20 μmol h^{-1}	[S5]
Nano TiO_2	CuO	3.5% NaCl (45 mL); 300 W Xe lamp (Full spectrum)	H_2: 0.31 μmol h^{-1}	[S6]
ZIS-P200	Ru	0.5 M NaCl (60 mL); 350 W Xe lamp ($\lambda > 400$ nm)	H_2: 3.43 μmol h^{-1}	This work
CdS	CoS	0.55 M NaCl with 0.2 M Na_2S/Na_2SO_3 (6 mL); Visible light ($\lambda > 420$ nm)	H_2: 1.43 μmol h^{-1}	[S7]

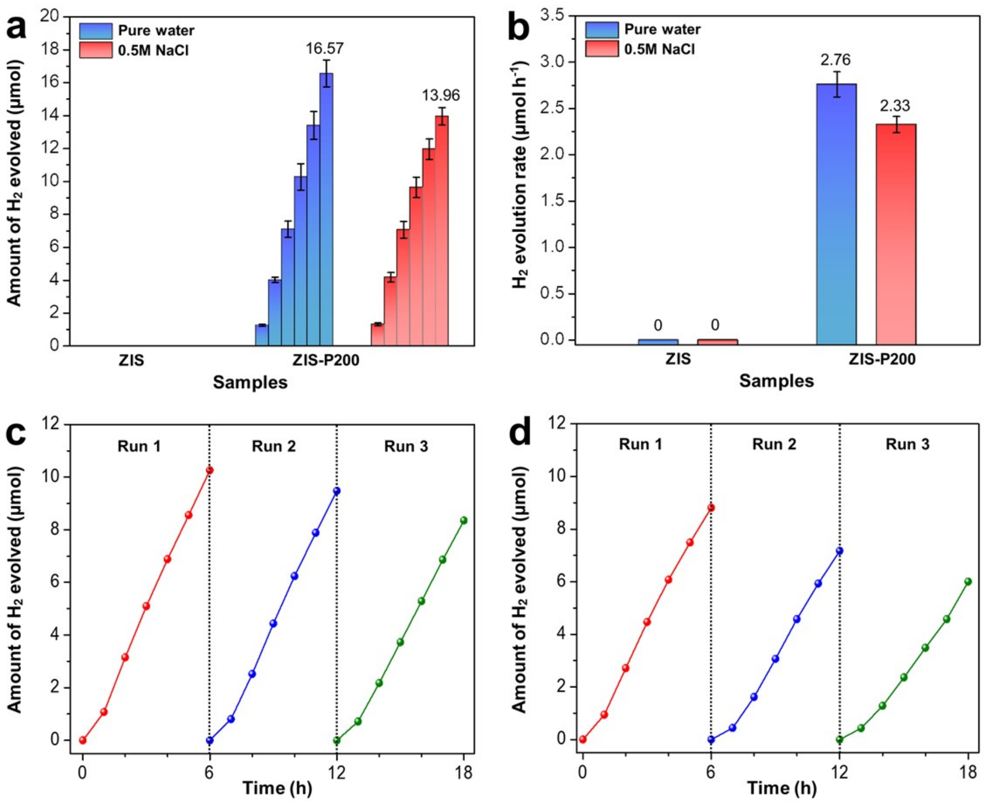

Fig. S7 Photocatalytic performance under full spectrum irradiation. (a) Time courses of H_2 evolution and (b) corresponding H_2 yield of ZIS and ZIS-P200 in pure water and 0.5 M NaCl under full spectrum irradiation. Recycling runs of photocatalytic H_2 evolution for ZIS-P200 in (c) pure water and (d) 0.5 M NaCl under visible light irradiation.

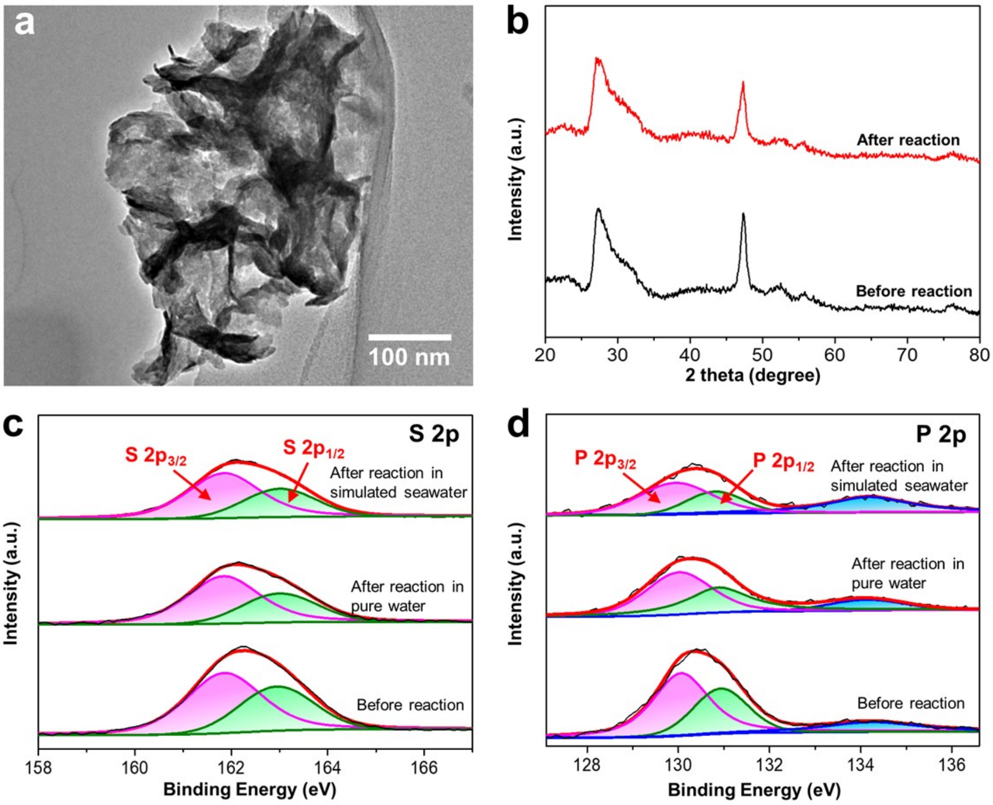

Fig. S8 Photocatalytic stability analysis. (a) Representative TEM image of ZIS-P200 after three repeated photocatalytic cycles in pure water. (b) XRD patterns, (c) S 2p and (d) P 2p XPS spectra of ZIS-P200 before and after three repeated photocatalytic cycles in pure water and simulated seawater.

Table S5. Relative atomic ratio of ZIS-P200 before and after three repeated photocatalytic cycles in pure water and simulated seawater measured by XPS.

Sample	**Atomic Ratio (Normalized to Zn = 1)**			
	Zn	In	S	P
Before reaction	1	2.19	3.30	0.50
After reaction in pure water	1	2.07	3.06	0.47
After reaction in simulated seawater	1	2.00	2.96	0.43

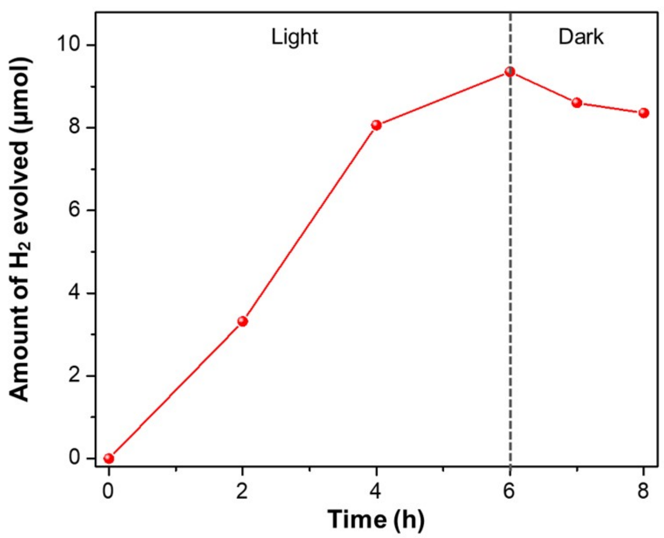

Fig. S9 Backward reaction testing. Time courses of H_2 evolution of ZIS-P200 in pure water under visible light irradiation and dark condition.

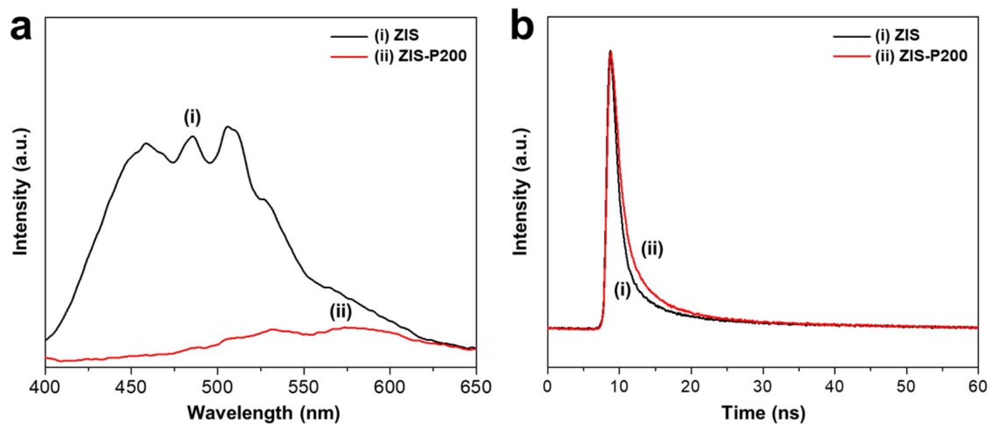

Fig. S10 Photoluminescence analysis. (a) Steady-state PL spectra and (b) time-resolved PL decay curves of (i) ZIS and (ii) ZIS-P200.

References

[S1] Shi, X.; Mao, L.; Dai, C.; Yang, P.; Zhang, J.; Dong, F.; Zheng, L.; Fujitsuka, M.; Zheng, H., Inert basal plane activation of two-dimensional $ZnIn_2S_4$ via Ni atom doping for enhanced co-catalyst free photocatalytic hydrogen evolution. *J. Mater. Chem. A* **2020,** *8* (26), 13376-13384.

[S2] Ng, B.-J.; Putri, L. K.; Kong, X. Y.; Pasbakhsh, P.; Chai, S.-P., Overall pure water splitting using one-dimensional P-doped twinned $Zn_{0.5}Cd_{0.5}S_{1-x}$ nanorods via synergetic combination of long-range ordered homojunctions and interstitial S vacancies with prolonged carrier lifetime. *Appl. Catal. B* **2020,** *262*, 118309.

[S3] Zhong, Y.; Wu, Y.; Chang, B.; Ai, Z.; Zhang, K.; Shao, Y.; Zhang, L.; Hao, X., A CoP/CdS/WS_2 p–n–n tandem heterostructure: a novel photocatalyst for hydrogen evolution without using sacrificial agents. *J. Mater. Chem. A* **2019,** *7* (24), 14638-14645.

[S4] Shi, R.; Ye, H.-F.; Liang, F.; Wang, Z.; Li, K.; Weng, Y.; Lin, Z.; Fu, W.-F.; Che, C.-M.; Chen, Y., Interstitial P-doped CdS with long-lived photogenerated electrons for photocatalytic water splitting without sacrificial agents. *Adv. Mater.* **2018,** *30*, 1705941.

[S5] Cui, G.; Wang, W.; Ma, M.; Xie, J.; Shi, X.; Deng, N.; Xin, J.; Tang, B., IR-driven ohotocatalytic water splitting with WO_2-Na_xWO_3 hybrid conductor material. *Nano Lett.* **2015,** *15* (11), 7199-7203.

[S6] Simamora, A. J.; Hsiung, T. L.; Chang, F. C.; Yang, T. C.; Liao, C. Y.; Wang, H. P., Photocatalytic splitting of seawater and degradation of methylene blue on CuO/nano TiO_2. *Int. J. Hydrogen Energy* **2012,** *37* (18), 13855-13858.

[S7] Liu, S.; Ma, Y.; Chi, D.; Sun, Y.; Chen, Q.; Zhang, J.; He, Z.; He, L.; Zhang, K.; Liu, B., Hollow heterostructure CoS/CdS photocatalysts with enhanced charge transfer for photocatalytic hydrogen production from seawater. *Int. J. Hydrogen Energy* **2022,** *47* (15), 9220-9229.